arXiv:1201.1498v1 [math.PR] 6 Jan 2012

Imaginary geometry III: reversibility of SLE_κ for $\kappa \in (4,8)$

Jason Miller and Scott Sheffield

Abstract

Suppose that $D \subseteq \mathbf{C}$ is a Jordan domain and $x, y \in \partial D$ are distinct. Fix $\kappa \in (4,8)$ and let η be an SLE_κ process from x to y in D. We prove that the law of the time-reversal of η is, up to reparameterization, an SLE_κ process from y to x in D. More generally, we prove that $\mathrm{SLE}_\kappa(\rho_1;\rho_2)$ processes are reversible if and only if both ρ_i are at least $\kappa/2-4$, which is the critical threshold at or below which such curves are boundary filling.

Our result supplies the missing ingredient needed to show that for all $\kappa \in (4,8)$ the so-called *conformal loop ensembles* CLE_κ are canonically defined, with almost surely continuous loops. It also provides an interesting way to couple two Gaussian free fields (with different boundary conditions) so that their difference is piecewise constant and the boundaries between the constant regions are SLE_κ curves.

Contents

1 Introduction **3**

2 Preliminaries **8**
2.1 SLE$_\kappa(\rho)$ Processes 8
2.2 Imaginary Geometry of the Gaussian Free Field 9

3 Proofs **18**
3.1 Reducing Theorems 1.1 and 1.2 to critical case 20
3.2 Main lemma 20
3.3 Iteration procedure exhausts curve 25
3.4 Non-critical boundary-filling paths 29

4 Couplings **29**

Acknowledgments. We thank David Wilson and Dapeng Zhan for helpful discussions.

1 Introduction

Fix $\kappa \in (2,4)$ and write $\kappa' = 16/\kappa \in (4,8)$. Our main result is the following:

Theorem 1.1. *Suppose that D is a Jordan domain and let $x, y \in \partial D$ be distinct. Let η' be a chordal $\mathrm{SLE}_{\kappa'}$ process in D from x to y. Then the law of η' has time-reversal symmetry. That is, if $\psi \colon D \to D$ is an anti-conformal map which swaps x and y, then the time-reversal of $\psi \circ \eta'$ is equal in law to η', up to reparameterization.*

Since chordal SLE_κ curves were introduced by Schramm in 1999 [21], they have been widely believed and conjectured to be time-reversible for all $\kappa \leq 8$. For certain κ values, this follows from the fact that SLE_κ is a scaling limit of a discrete model that does not distinguish between paths from x to y and paths from y to x ($\kappa = 2$: chordal loop-erased random walk [11], $\kappa = 3$: Ising model spin cluster boundaries [30], $\kappa = 4$: level lines of the discrete Gaussian free field [24], $\kappa = 16/3$: the FK-Ising model cluster boundaries [30], $\kappa = 6$: critical percolation [29, 2], $\kappa = 8$ uniform spanning tree boundary [11]).

The reversibility of chordal SLE_κ curves for arbitrary $\kappa \in (0,4]$ was established by Zhan [32] in a landmark work that builds on the commutativity approach proposed by Dubédat [4] and by Schramm [21] in order to show that it is possible to construct a coupling of two SLE_κ curves growing at each other in opposite directions so that their ranges are almost surely equal. By expanding on this approach, Dubédat [5] and Zhan [33] extended this result to include one-sided $\mathrm{SLE}_\kappa(\rho)$ processes with $\kappa \in (0,4]$ which do not intersect the boundary (i.e., $\rho \geq \frac{\kappa}{2} - 2$). The reversibility of the entire class of chordal $\mathrm{SLE}_\kappa(\rho_1;\rho_2)$ processes for $\rho_1, \rho_2 > -2$ (even when they intersect the boundary) was proved in [16] using a different approach, based on coupling SLE with the Gaussian free field [15].

This work is a sequel to and makes heavy use of the techniques and results from [15, 16]. We summarize these results in Section 2.2, so that this work can be read independently. Of particular importance is a variant of the “light cone” characterization of $\mathrm{SLE}_{\kappa'}$ traces given in [15], which is a refinement of so-called Duplantier duality. This gives a description of the outer boundary of an $\mathrm{SLE}_{\kappa'}$ process stopped upon hitting the boundary in terms of a certain

SLE_κ process. We will also employ the almost sure continuity of so-called $\mathrm{SLE}_\kappa(\underline{\rho})$ and $\mathrm{SLE}_{\kappa'}(\underline{\rho}')$ traces (see Section 2.2), even when they interact non-trivially with the boundary [15, Theorem 1.3].

Theorem 1.1 is a special case of a more general theorem which gives the time-reversal symmetry of $\mathrm{SLE}_{\kappa'}(\rho_1;\rho_2)$ processes provided $\rho_1,\rho_2 \geq \frac{\kappa'}{2}-4$. We remark that the value $\frac{\kappa'}{2}-4$ is the critical threshold at or below which such processes are boundary filling [15].

Theorem 1.2. *Suppose that D is a Jordan domain and let $x,y \in \partial D$ be distinct. Suppose that η' is a chordal $\mathrm{SLE}_{\kappa'}(\rho_1;\rho_2)$ process in D from x to y where the force points are located at x^- and x^+. If $\psi\colon D \to D$ is an anti-conformal map which swaps x and y, then the time-reversal of $\psi \circ \eta'$ is an $\mathrm{SLE}_{\kappa'}(\rho_1;\rho_2)$ process from x to y, up to reparameterization.*

Theorem 1.2 has many consequences for SLE. For example, the *conformal loop ensembles* CLE_κ are random collections of loops in a planar domain, defined for all $\kappa \in (8/3,8]$. Each loop in a CLE_κ looks locally like SLE_κ, and the collection of loops can be constructed using a branching form of $\mathrm{SLE}_\kappa(\kappa-6)$ that traces through all of the loops, as described in [28]. However, there is some arbitrariness in the construction given in [28]: one has to choose a boundary point at which to start this process, and it was not clear in [28] whether the law of the final loop collection was independent of this initial choice; also, each loop is traced from a specific starting/ending point, and it was not clear that the "loops" thus constructed were actually continuous at this point.

For $\kappa \in (4,8]$ the continuity and initial-point independence were proved in [28] as results *contingent* on the continuity and time-reversal symmetry of SLE_κ and $\mathrm{SLE}_\kappa(\kappa-6)$ processes. As mentioned above, continuity was recently established in [15]; thus Theorem 1.2 implies that the CLE_κ defined in [28] are almost surely ensembles of continuous loops and that their laws are indeed canonical (independent of the location at which the branching form of $\mathrm{SLE}_\kappa(\kappa-6)$ is started). We remark that the analogous fact for CLE_κ with $\kappa \in (8/3,4]$ was only recently proved in [27]. In that case, the continuity and initial-point independence are established by showing that the branching $\mathrm{SLE}_\kappa(\kappa-6)$ construction of CLE_κ is equivalent to the *loop-soup-cluster-boundary* construction proposed by Werner.

Our final result is the non-reversibility of $\mathrm{SLE}_{\kappa'}(\rho_1;\rho_2)$ processes when either $\rho_1 < \frac{\kappa'}{2}-4$ or $\rho_2 < \frac{\kappa'}{2}-4$:

Theorem 1.3. *Suppose that D is a Jordan domain and let $x, y \in \partial D$ be distinct. Suppose that η' is a chordal* $\mathrm{SLE}_{\kappa'}(\rho_1;\rho_2)$ *process in D from x to y. Let $\psi\colon D \to D$ be an anti-conformal map which swaps x and y. If either $\rho_1 < \frac{\kappa'}{2} - 4$ or $\rho_2 < \frac{\kappa'}{2} - 4$, then the law of the time-reversal of $\psi(\eta')$ is not an* $\mathrm{SLE}_{\kappa'}(\underline{\rho})$ *process for any collection of weights $\underline{\rho}$.*

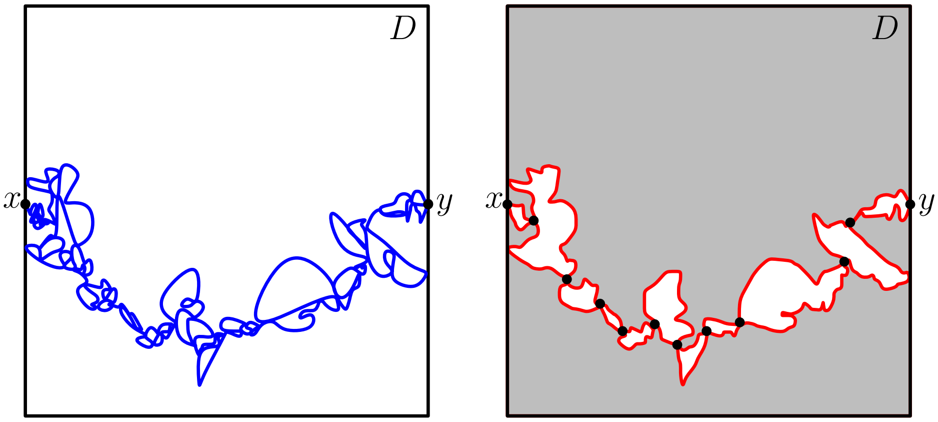

Figure 1.1: The curve on the left represents an $\mathrm{SLE}_{\kappa'}(\rho_1;\rho_2)$ where $\kappa' \in (4,8)$ and $\rho_1, \rho_2 \geq \frac{\kappa'}{2} - 4$. It was shown in [15, Theorem 1.4] and [16, Theorem 1.1] that the law of the outer boundary of this path (the pair of red curves from x to y on the right) has time-reversal symmetry; thus one can couple an $\mathrm{SLE}_{\kappa'}(\rho_1;\rho_2)$ path η' from x to y with an $\mathrm{SLE}_{\kappa'}(\rho_2;\rho_1)$ path γ' from y to x in such a way that their boundaries almost surely agree. Moreover, it was also shown in [15, Proposition 7.30] that *given* these outer boundaries, the conditional law of the path within each of the white "bubbles" shown on the right (i.e., each of the countably many components of the complement of the boundary that lies between the two boundary paths) is given by an independent $\mathrm{SLE}_{\kappa'}(\frac{\kappa'}{2} - 4; \frac{\kappa'}{2} - 4)$ process from its first to its last endpoint (illustrated by the black dots on the right). Thus, if $\mathrm{SLE}_{\kappa'}(\frac{\kappa'}{2} - 4; \frac{\kappa'}{2} - 4)$ has time-reversal symmetry, then we can couple η' and γ' so that they agree (up to time-reversal) within each bubble as well.

Outline

The remainder of this article is structured as follows. In Section 2, we will give a brief overview of both SLE and the so-called imaginary geometry of the Gaussian free field. The latter is a non-technical summary of the results proved in [15] which are needed for this article. This section is similar to [16, Section 2]. In Section 3, we will prove Theorems 1.1-1.3. Finally, in Section 4 we briefly explain how these theorems can be used to construct couplings of different Gaussian free field instances with different boundary conditions; as an application, we compute a simple formula for the probability that a given point lies to the left of an $\mathrm{SLE}_{\kappa'}(\frac{\kappa'}{2}-4;\frac{\kappa'}{2}-4)$ curve. (The analogous result for $\mathrm{SLE}_{\kappa'}$, computed by Schramm in [22], does not have such a simple form.)

As Figure 1.1 illustrates, when $\kappa' \in (4,8)$ and $\rho_1, \rho_2 \geq \frac{\kappa'}{2}-4$, the results obtained in [15, 16] reduce the problem of showing time-reversal symmetry to the special case that η' is an $\mathrm{SLE}_{\kappa'}(\frac{\kappa'}{2}-4;\frac{\kappa'}{2}-4)$, which is a random curve that hits every point on the entire boundary almost surely. The second step is to pick some point z on the boundary of D and consider the outer boundaries of the *past* and *future* of η' upon hitting z — i.e., the outer boundary of the set of points visited by η' before hitting z and the outer boundary of the set of points visited by η' after hitting z, as illustrated in Figure 1.2. Lemma 3.2 shows that the law of this pair of paths is invariant under the anti-conformal map $D \to D$ that swaps x and y while fixing z.

The proof of Lemma 3.2 is the heart of the argument. It makes use of Gaussian free field machinery in a rather picturesque way that avoids the need for extensive calculations. Roughly speaking, we will first consider an "infinite volume limit" obtained by "zooming in" near the point z in Figure 1.2. In this limit, we find a coupled pair of $\mathrm{SLE}_{\kappa}(\rho_1;\rho_2)$ paths from $z \in \partial \mathbf{H}$ to ∞ in $\mathbf{H}$ and [16, Theorem 1.1] implies that the law of the pair of paths is invariant under reflection about the vertical axis through z. By employing a second trick (involving a second pair of paths started at a second point in $\partial \mathbf{H}$) we are able to recover the finite volume symmetry from the infinite volume symmetry.

Once we have Lemma 3.2, we can couple forward and reverse $\mathrm{SLE}_{\kappa'}(\frac{\kappa'}{2}-4;\frac{\kappa'}{2}-4)$ processes so that their past and future upon hitting z have the same outer boundaries. Moreover, given the information in Figure 1.2, [15, Proposition 7.32] implies that the conditional law of η' within each of these bubbles is again an independent $\mathrm{SLE}_{\kappa'}(\frac{\kappa'}{2}-4;\frac{\kappa'}{2}-4)$ process. (This is a

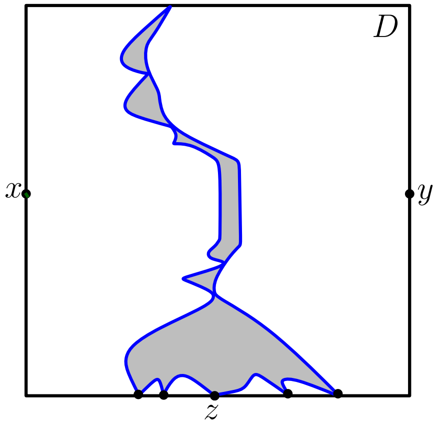

Figure 1.2: Let η' be an $\mathrm{SLE}_{\kappa'}(\frac{\kappa'}{2}-4;\frac{\kappa'}{2}-4)$ (which almost surely hits every point on ∂D) and let z be a fixed point on ∂D. The left of the two blue curves shown (starting at z, ending at the top of the box) is the outer boundary of the "past of z" (i.e., the set of all points η' disconnects from y before z is hit). The right blue curve with the same endpoints is the outer boundary of the "future of z" (i.e., the set of all points the time-reversal of η' disconnects from x before z is hit). Lemma 3.2 shows that the law of this pair of paths is invariant under the anti-conformal map $D \to D$ that swaps x and y while fixing z. Thus we can couple forward and reverse $\mathrm{SLE}_{\kappa'}(\frac{\kappa'}{2}-4;\frac{\kappa'}{2}-4)$ processes so that these boundaries are the same for both of them. The conditional law of η' within each of the white bubbles is given by an independent $\mathrm{SLE}_{\kappa'}(\frac{\kappa'}{2}-4;\frac{\kappa'}{2}-4)$ process [15, Proposition 7.24], so we can iterate this construction.

consequence of the "light cone" characterization of $\mathrm{SLE}_{\kappa'}$ processes established in [15].) Thus we can pick any point on the boundary of a bubble and further couple so that the past and future of that point (within the bubble) have the same boundary. Iterating this procedure a countably infinite number of times allows us to couple two $\mathrm{SLE}_{\kappa'}(\frac{\kappa'}{2}-4;\frac{\kappa'}{2}-4)$ curves so that one is almost surely the time-reversal of the other, thereby proving Theorem 1.2. The non-reversibility when one of ρ_1 or ρ_2 is less than $\frac{\kappa'}{2}-4$ is shown by checking that the analog of Figure 1.2 is *not* invariant under anti-conformal maps (fixing z, swapping x and y) in this case.

2 Preliminaries

The purpose of this section is to review the basic properties of $\text{SLE}_\kappa(\underline{\rho}^L;\underline{\rho}^R)$ processes in addition to giving a non-technical overview of the so-called imaginary geometry of the Gaussian free field. The latter is a mechanism for constructing couplings of many $\text{SLE}_\kappa(\underline{\rho}^L;\underline{\rho}^R)$ strands in such a way that it is easy to compute the conditional law of one of the curves given the realization of the others [15].

2.1 $\text{SLE}_\kappa(\rho)$ Processes

SLE_κ is a one-parameter family of conformally invariant random curves, introduced by Oded Schramm in [21] as a candidate for (and later proved to be) the scaling limit of loop erased random walk [11] and the interfaces in critical percolation [29, 2]. Schramm's curves have been shown so far also to arise as the scaling limit of the macroscopic interfaces in several other models from statistical physics: [24, 30, 3, 23, 14]. More detailed introductions to SLE can be found in many excellent survey articles of the subject, e.g., [31, 10].

An SLE_κ in $\mathbf{H}$ from 0 to ∞ is defined by the random family of conformal maps g_t obtained by solving the Loewner ODE

$$\partial_t g_t(z) = \frac{2}{g_t(z) - W_t}, \quad g_0(z) = z \tag{2.1}$$

where $W = \sqrt{\kappa} B$ and B is a standard Brownian motion. Write $K_t := \{z \in \mathbf{H} : \tau(z) \leq t\}$. Then g_t is a conformal map from $\mathbf{H}_t := \mathbf{H} \setminus K_t$ to $\mathbf{H}$ satisfying $\lim_{|z|\to\infty} |g_t(z) - z| = 0$.

Rohde and Schramm showed that there almost surely exists a curve η (the so-called SLE *trace*) such that for each $t \geq 0$ the domain $\mathbf{H}_t$ is the unbounded connected component of $\mathbf{H} \setminus \eta([0,t])$, in which case the (necessarily simply connected and closed) set K_t is called the "filling" of $\eta([0,t])$ [19]. An SLE_κ connecting boundary points x and y of an arbitrary simply connected Jordan domain can be constructed as the image of an SLE_κ on $\mathbf{H}$ under a conformal transformation $\psi\colon \mathbf{H} \to D$ sending 0 to x and ∞ to y. (The choice of ψ does not affect the law of this image path, since the law of SLE_κ on $\mathbf{H}$ is scale invariant.) SLE_κ is characterized by the fact that it satisfies the domain Markov property and is invariant under conformal transformations.

$\mathrm{SLE}_\kappa(\underline{\rho}^L;\underline{\rho}^R)$ is the stochastic process one obtains by solving (2.1) where the driving function W is taken to be the solution to the SDE

$$\begin{aligned} dW_t &= \sqrt{\kappa}dB_t + \sum_{q\in\{L,R\}} \sum_i \frac{\rho^{i,q}}{W_t - V_t^{i,q}} dt \\ dV_t^{i,q} &= \frac{2}{V_t^{i,q} - W_t} dt, \quad V_0^{i,q} = x^{i,q}. \end{aligned} \tag{2.2}$$

Like SLE_κ, the $\mathrm{SLE}_\kappa(\underline{\rho}^L;\underline{\rho}^R)$ processes arise in a variety of natural contexts. The existence and uniqueness of solutions to (2.2) is discussed in [15, Section 2]. In particular, it is shown that there is a unique solution to (2.2) until the first time t that $W_t = V_t^{j,q}$ where $\sum_{i=1}^j \rho^{i,q} \leq -2$ for $q \in \{L,R\}$ — we call this time the **continuation threshold** (see [15, Section 2]). In particular, if $\sum_{i=1}^j \rho^{i,q} > -2$ for all $1 \leq j \leq |\underline{\rho}^q|$ for $q \in \{L,R\}$, then (2.2) has a unique solution for all times t. This even holds when one or both of the $x^{1,q}$ are zero. The almost sure continuity of the $\mathrm{SLE}_\kappa(\underline{\rho}^L;\underline{\rho}^R)$ trace is also proved in [15, Theorem 1.3].

2.2 Imaginary Geometry of the Gaussian Free Field

We will now give an overview of the so-called *imaginary geometry* of the Gaussian free field (GFF). In this article, this serves as a tool for constructing couplings of multiple SLE strands and provides a simple calculus for computing the conditional law of one of the strands given the realization of the others [15]. The purpose of this overview is to explain just enough of the theory so that this article may read and understood independently of [15], however we refer the reader interested in proofs of the statements we make here to [15]. We begin by fixing a domain $D \subseteq \mathbf{C}$ with smooth boundary and letting $C_0^\infty(D)$ denote the space of compactly supported C^∞ functions on D. For $f, g \in C_0^\infty(D)$, we let

$$(f,g)_\nabla := \frac{1}{2\pi} \int_D \nabla f(x) \cdot \nabla g(x) dx$$

denote the Dirichlet inner product of f and g where dx is the Lebesgue measure on D. Let $H(D)$ be the Hilbert space closure of $C_0^\infty(D)$ under $(\cdot,\cdot)_\nabla$. The continuum Gaussian free field h (with zero boundary conditions) is the so-called standard Gaussian on $H(D)$. It is given formally as a random linear combination

$$h = \sum_n \alpha_n f_n, \tag{2.3}$$

where (α_n) are i.i.d. $N(0,1)$ and (f_n) is an orthonormal basis of $H(D)$. The GFF with non-zero boundary data ψ is given by adding the harmonic extension of ψ to a zero-boundary GFF h.

The GFF is a two-dimensional-time analog of Brownian motion. Just as Brownian motion can be realized as the scaling limit of many random lattice walks, the GFF arises as the scaling limit of many random (real or integer valued) functions on two dimensional lattices [1, 9, 17, 18, 13]. The GFF can be used to generate various kinds of random geometric structures, in particular the imaginary geometry discussed here [26, 15]. This corresponds to considering $e^{ih/\chi}$, for a fixed constant $\chi > 0$. Informally, the "rays" of the imaginary geometry are flow lines of the complex vector field $e^{i(h/\chi+\theta)}$, i.e., solutions to the ODE

$$\eta'(t) = e^{i(h(\eta(t))+\theta)} \text{ for } t > 0, \tag{2.4}$$

for given values of $\eta(0)$ and θ.

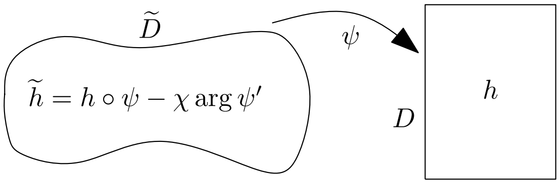

Figure 2.1: The set of flow lines in $\widetilde{D}$ is the pullback via a conformal map ψ of the set of flow lines in D provided h is transformed to a new function $\widetilde{h}$ in the manner shown.

A brief overview of imaginary geometry (as defined for general functions h) appears in [26], where the rays are interpreted as geodesics of a variant of the Levi-Civita connection associated with Liouville quantum gravity. One can interpret the e^{ih} direction as "north" and the $e^{i(h+\pi/2)}$ direction as "west", etc. Then h determines a way of assigning a set of compass directions to every point in the domain, and a ray is determined by an initial point and a direction. When h is constant, the rays correspond to rays in ordinary Euclidean geometry. For more general continuous h, one can still show that when three rays form a triangle, the sum of the angles is always π [26].

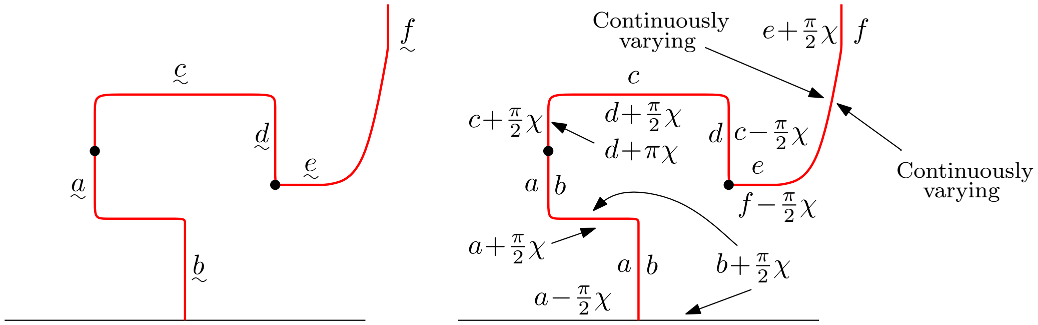

Figure 2.2: We will often make use of the notation depicted on the left hand side to indicate boundary values for Gaussian free fields. Specifically, we will delineate the boundary ∂D of a Jordan domain D with black dots. On each arc L of ∂D which lies between a pair of black dots, we will draw either a horizontal or vertical segment L_0 and label it with $\underset{\sim}{x}$. This means that the boundary data on L_0 is given by x. Whenever L makes a quarter turn to the right, the height goes down by $\frac{\pi}{2}\chi$ and whenever L makes a quarter turn to the left, the height goes up by $\frac{\pi}{2}\chi$. More generally, if L makes a turn which is not necessarily at a right angle, the boundary data is given by χ times the winding of L relative to L_0. If we just write x next to a horizontal or vertical segment, we mean to indicate the boundary data just at that segment and nowhere else. The right side above has exactly the same meaning as the left side, but the boundary data is spelled out explicitly everywhere. Even when the curve has a fractal, non-smooth structure, the *harmonic extension* of the boundary values still makes sense, since one can transform the figure via the rule in Figure 2.1 to a half plane with piecewise constant boundary conditions.

To build these rays, one begins by constructing explicit couplings of h with variants of SLE and showing that these couplings have certain properties. Namely, if one conditions on part of the curve, then the conditional law of h is that of a GFF in the complement of the curve with certain boundary conditions (see Figure 2.3). Examples of these couplings appear in [25, 20, 6, 26] as well as variants in [12, 7, 8]. The next step is to show that in these couplings the path is almost surely *determined by the field* so that we can really interpret the ray as a path-valued function of the field. This step is carried out in some generality in [6, 26, 15].

If h is a smooth function, η a flow line of $e^{ih/\chi}$, and $\psi\colon \widetilde{D} \to D$ a conformal transformation, then by the chain rule, $\psi^{-1}(\eta)$ is a flow line of $h\circ\psi - \chi \arg \psi'$, as in Figure 2.1. With this in mind, we define an **imaginary surface** to be an equivalence class of pairs (D,h) under the equivalence relation

$$(D,h) \to (\psi^{-1}(D), h\circ\psi - \chi \arg\psi') = (\widetilde{D},\widetilde{h}). \tag{2.5}$$

We interpret ψ as a (conformal) *coordinate change* of the imaginary surface. In what follows, we will generally take D to be the upper half plane, but one can map the flow lines defined there to other domains using (2.5).

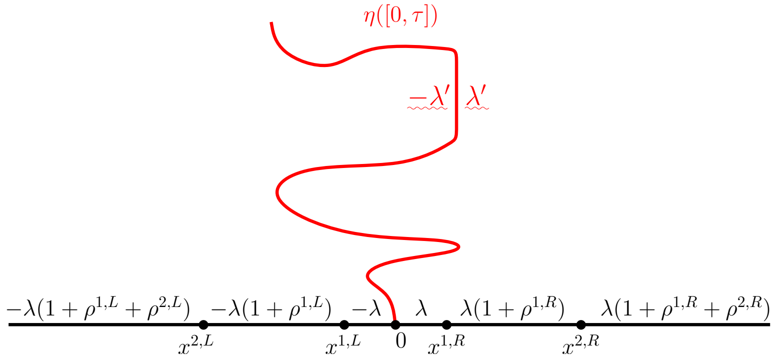
$\eta([0,\tau])$
$\underset{\sim}{-\lambda'}$
$\underset{\sim}{\lambda'}$
$-\lambda(1+\rho^{1,L}+\rho^{2,L})$
$-\lambda(1+\rho^{1,L})$
$-\lambda$
λ
$\lambda(1+\rho^{1,R})$
$\lambda(1+\rho^{1,R}+\rho^{2,R})$
$x^{2,L}$
$x^{1,L}$
0
$x^{1,R}$
$x^{2,R}$

Figure 2.3: Suppose that h is a GFF on $\mathbf{H}$ with the boundary data depicted above. Then the flow line η of h starting from 0 is an $\mathrm{SLE}_\kappa(\underline{\rho}^L;\underline{\rho}^R)$ curve in $\mathbf{H}$ where $|\underline{\rho}^L| = |\underline{\rho}^R| = 2$. Conditional on $\eta([0,\tau])$ for any η stopping time τ, h is equal in distribution to a GFF on $\mathbf{H}\setminus\eta([0,\tau])$ with the boundary data on $\eta([0,\tau])$ depicted above (the notation $\underset{\sim}{a}$ which appears adjacent to $\eta([0,\tau])$ is explained in some detail in Figure 2.2). It is also possible to couple $\eta' \sim \mathrm{SLE}_{\kappa'}(\underline{\rho}^L;\underline{\rho}^R)$ for $\kappa' > 4$ with h and the boundary data takes on the same form. The difference is in the interpretation — η' is not a flow line of h, but for each time τ, the left and right outer boundaries of the set $\eta'([0,\tau])$, traced starting from $\eta(\tau)$, are flow lines of h with appropriate angles.

We assume throughout the rest of this section that $\kappa \in (0,4)$ so that $\kappa' := 16/\kappa \in (4,\infty)$. When following the illustrations, it will be useful to keep in mind a few definitions and identities:

$$\lambda := \frac{\pi}{\sqrt{\kappa}}, \qquad \lambda' := \frac{\pi}{\sqrt{16/\kappa}} = \frac{\pi\sqrt{\kappa}}{4} = \frac{\kappa}{4}\lambda < \lambda, \qquad \chi := \frac{2}{\sqrt{\kappa}} - \frac{\sqrt{\kappa}}{2} > 0 \tag{2.6}$$

$$2\pi\chi = 4(\lambda - \lambda'), \qquad \lambda' = \lambda - \frac{\pi}{2}\chi \tag{2.7}$$

$$2\pi\chi = (4-\kappa)\lambda = (\kappa'-4)\lambda'. \tag{2.8}$$

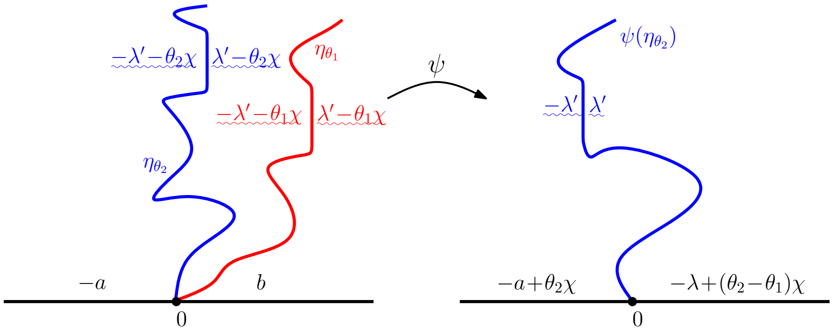

Figure 2.4: Suppose that h is a GFF on $\mathbf{H}$ with the boundary data depicted above. For each $\theta \in \mathbf{R}$, let η_θ be the flow line of the GFF $h + \theta\chi$. This corresponds to setting the initial angle of η_θ to be θ. Just as if h were a smooth function, if $\theta_1 < \theta_2$ then η_{θ_1} lies to the right of η_{θ_2} [15, Theorem 1.5]. The conditional law of h given η_{θ_1} and η_{θ_2} is a GFF on $\mathbf{H} \setminus \cup_{i=1}^2 \eta_{\theta_i}$ whose boundary data is shown above [15, Proposition 6.1]. By applying a conformal mapping and using the transformation rule (2.5), we can compute the conditional law of η_{θ_1} given the realization of η_{θ_2} and vice-versa. That is, η_{θ_2} given η_{θ_1} is an $\mathrm{SLE}_\kappa((a-\theta_2\chi)/\lambda - 1; (\theta_2-\theta_1)\chi/\lambda - 2)$ process independently in each of the connected components of $\mathbf{H} \setminus \eta_{\theta_1}$ which lie to the left of η_{θ_1}. Moreover, η_{θ_1} given η_{θ_2} is an $\mathrm{SLE}_\kappa((\theta_2-\theta_1)\chi/\lambda - 2; (b+\theta_1\chi)/\lambda - 1)$ independently in each of the connected components of $\mathbf{H} \setminus \eta_{\theta_2}$ which lie to the right of η_{θ_2} [15, Section 7.1].

The boundary data one associates with the GFF on $\mathbf{H}$ so that its flow line from 0 to ∞ is an $\mathrm{SLE}_\kappa(\underline{\rho}^L; \underline{\rho}^R)$ process with force points located at $\underline{x} = (\underline{x}^L, \underline{x}^R)$ is

$$-\lambda\left(1 + \sum_{i=1}^{j} \rho^{i,L}\right) \quad \text{for } x \in [x^{j+1,L}, x^{j,L}) \text{ and} \tag{2.9}$$

$$\lambda\left(1 + \sum_{i=1}^{j} \rho^{i,R}\right) \quad \text{for } x \in [x^{j,R}, x^{j+1,R}) \tag{2.10}$$

This is depicted in Figure 2.3 in the special case that $|\underline{\rho}^L| = |\underline{\rho}^R| = 2$. As we explained earlier, for any η stopping time τ, the law of h conditional on $\eta([0,\tau])$ is a GFF in $\mathbf{H} \setminus \eta([0,\tau])$. The boundary data of the conditional field agrees with that of h on $\partial \mathbf{H}$. On the right side of $\eta([0,\tau])$, it is $\lambda' + \chi \cdot \text{winding}$, where the terminology "winding" is explained in Figure 2.2, and to the left it is $-\lambda' + \chi \cdot \text{winding}$. This is also depicted in Figure 2.3.

By considering several flow lines of the same field, we can construct couplings of multiple $\text{SLE}_\kappa(\underline{\rho})$ processes. For example, suppose that $\theta \in \mathbf{R}$. The flow line η_θ of $h + \theta\chi$ should be interpreted as the flow line of the vector field $e^{ih/\chi + \theta}$. That is, η_θ is the flow line of h with initial angle θ. If h were a continuous function and we had $\theta_1 < \theta_2$, then it would be obvious that η_{θ_1} lies to the right of η_{θ_2}. Although non-trivial to prove, this is also true in the setting of the GFF [15, Theorem 1.5] and is depicted in Figure 2.4.

For $\theta_1 < \theta_2$, we can compute the conditional law of η_{θ_2} given η_{θ_1} [15, Section 7.1]. It is an $\text{SLE}_\kappa((a - \theta_2\chi)/\lambda - 1; (\theta_2 - \theta_1)\chi/\lambda - 2)$ process independently in each connected component of $\mathbf{H} \setminus \eta_{\theta_1}$ which lies to the left of η_{θ_1} [15, Section 7.1]. Moreover, η_{θ_1} given η_{θ_2} is independently an $\text{SLE}_\kappa((\theta_2 - \theta_1)\chi/\lambda - 2; (b + \theta_1\chi)/\lambda - 1)$ in each of the connected components of $\mathbf{H} \setminus \eta_{\theta_2}$ which lie to the right of η_{θ_2}. This is depicted in Figure 2.4.

It is also possible to determine which segments of the boundary a flow or counterflow line cannot hit. This is described in terms of the boundary data of the field in Figure 2.5 and proved in [15, Lemma 5.2] (this result gives the range of boundary data that η cannot hit, contingent on the almost sure continuity of η; this, in turn, is given in [15, Theorem 1.3]). This can be rephrased in terms of the weights $\underline{\rho}$: an $\text{SLE}_\kappa(\underline{\rho})$ process almost surely does not hit a boundary interval $(x^{i,R}, x^{i+1,R})$ (resp. $(x^{i+1,L}, x^i)$) if $\sum_{s=1}^{i} \rho^{s,R} \geq \frac{\kappa}{2} - 2$ (resp. $\sum_{s=1}^{i} \rho^{s,L} \geq \frac{\kappa}{2} - 2$). See [15, Remark 5.3].

Recall that $\kappa' = 16/\kappa \in (4,\infty)$. We refer to $\text{SLE}_{\kappa'}$ processes η' as *counterflow* lines. The left boundaries of $\eta'([0,\tau'])$, taken over a range of τ' values, form a tree structure comprised of SLE_κ flow lines which in some sense run orthogonal to η'. The right boundaries form a dual tree structure. We can construct couplings of SLE_κ and $\text{SLE}_{\kappa'}$ processes (flow lines and counterflow lines) within the same imaginary geometry [15, Theorem 1.4]. This is depicted in Figure 2.6 in the special case of a single flow line η_θ with angle θ emanating from x and targeted at y and a single counterflow line η' emanating from y. When $\theta > \frac{1}{\chi}(\lambda - \lambda') = \frac{\pi}{2}$, η_θ almost surely passes to the left of (though may hit the left boundary of) η' [15, Theorem 1.4 and Theorem 1.5].

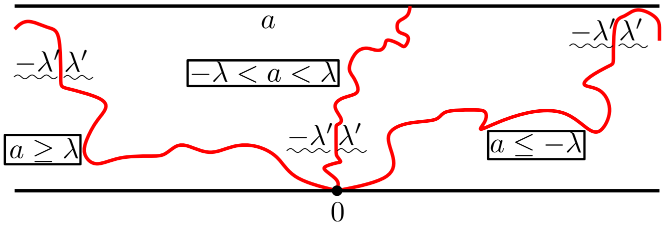

Figure 2.5: Suppose that h is a GFF on the strip $\mathcal{S}$ with the boundary data depicted above and η is the flow line of h starting at 0. The interaction of η with the upper boundary $\partial_U \mathcal{S}$ of $\partial \mathcal{S}$ depends on a, the boundary data of h on $\partial_U \mathcal{S}$. Curves shown represent almost sure behaviors corresponding to the three different regimes of a (indicated by the closed boxes). The path hits $\partial_U \mathcal{S}$ almost surely if and only if $a \in (-\lambda, \lambda)$. When $a \geq \lambda$, it tends to $-\infty$ (left end of the strip) and when $a \leq -\lambda$ it tends to ∞ (right end of the strip) without hitting $\partial_U \mathcal{S}$. This can be rephrased in terms of the weights $\underline{\rho}$: an $\mathrm{SLE}_\kappa(\underline{\rho})$ process almost surely does not hit a boundary interval $(x^{i,R}, x^{i+1,R})$ (resp. $(x^{i+1,L}, x^i)$) if $\sum_{s=1}^{i} \rho^{s,R} \geq \frac{\kappa}{2} - 2$ (resp. $\sum_{s=1}^{i} \rho^{s,L} \geq \frac{\kappa}{2} - 2$). See [15, Lemma 5.2] and [15, Remark 5.3]. These facts hold for all $\kappa > 0$.

If $\theta = \frac{\pi}{2}$, then η_θ is equal to the left boundary of η'. There is some intuition provided for this in Figure 2.6. Analogously, if $\theta < \frac{1}{\chi}(\lambda' - \lambda) = -\frac{\pi}{2}$, then η_θ passes to the right of η' [15, Theorem 1.4 and Theorem 1.5] and when $\theta = -\frac{\pi}{2}$, η_θ is equal to the right boundary of η'.

Just as in the setting of multiple flow lines, we can compute the conditional law of a counterflow line given the realization of a flow line (or multiple flow lines) within the same geometry. One case of this which will be particularly important for us is explained in Figure 2.7 — that the conditional law of η' given its left and right boundaries evolves as an $\mathrm{SLE}_{\kappa'}(\frac{\kappa'}{2} - 4; \frac{\kappa'}{2} - 4)$ process independently in each of the complementary connected components which lie between its left and right boundaries [15, Proposition 7.30]. This is sometimes referred to as "strong duality" for SLE (see [6, Section 8.2] for related results). We remark that $\frac{\kappa'}{2} - 4$ is the critical value of ρ at which counterflow lines are boundary filling. When $\rho > \frac{\kappa'}{2} - 4$, then $\mathrm{SLE}_{\kappa'}(\rho)$ does not fill the boundary and when $\rho \in (-2, \frac{\kappa'}{2} - 4]$, then $\mathrm{SLE}_{\kappa'}(\rho)$ does fill the boundary. The situation is analogous for two-sided $\mathrm{SLE}_{\kappa'}(\rho_1; \rho_2)$.

There is an important variant of SLE duality which allows us to give

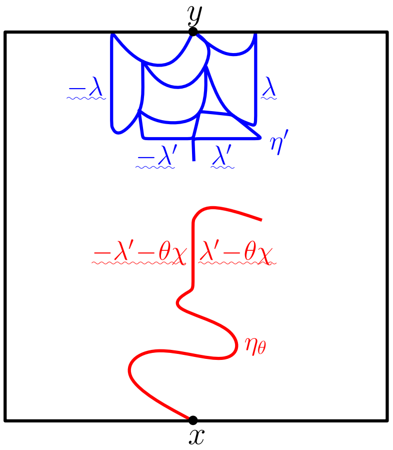

Figure 2.6: We can construct SLE_κ flow lines and $\mathrm{SLE}_{\kappa'}$, $\kappa' = 16/\kappa \in (4,\infty)$, counterflow lines within the same geometry. This is depicted above for a single counterflow line η' emanating from y and a flow line η_θ with angle θ starting from 0 (we intentionally did not describe the boundary data of h on ∂D). If $\theta = \theta_R := \frac{1}{\chi}(\lambda' - \lambda) = -\frac{\pi}{2}$ so that the boundary data on the right side of η_θ matches that on the right side of η', then η_θ will almost surely hit and then "merge" into the right boundary of $\eta'([0,\tau'])$ for any η' stopping time τ' and, more generally, the right boundary of the entire trace of η' is given by η_θ — this fact is known as SLE duality. Analogously, if $\theta = \theta_L := \frac{1}{\chi}(\lambda - \lambda') = \frac{\pi}{2} = -\theta_R$, then η_θ will almost surely hit and then merge into the left boundary of $\eta'([0,\tau'])$ and is equal to the left boundary of the entire trace of η'. These facts are proved in [15, Theorem 1.4].

the law of the outer boundary of the counterflow line η' upon hitting any point z on the boundary [15, Proposition 7.32]. If z is on the left side of ∂D, it is given by the flow line of h with angle $-\frac{\pi}{2}$ and if z is on the right side of ∂D, it is given by the flow of h with angle $\frac{\pi}{2}$. This is explained in Figure 2.8 in the special case of boundary filling $\mathrm{SLE}_{\kappa'}(\frac{\kappa'}{2} - 4; \frac{\kappa'}{2} - 4)$ processes. This will be particularly important for this article, since it will allow us to describe the geometry of the outer boundary between the set of points that η' visits before and after hitting a given boundary point. Iterating the procedure of decomposing the path into its future and past leads to a new path decomposition of $\mathrm{SLE}_{\kappa'}$ curves. We remark that this result is closely related to a decomposition of $\mathrm{SLE}_{\kappa'}$ paths into a so-called "light cone"

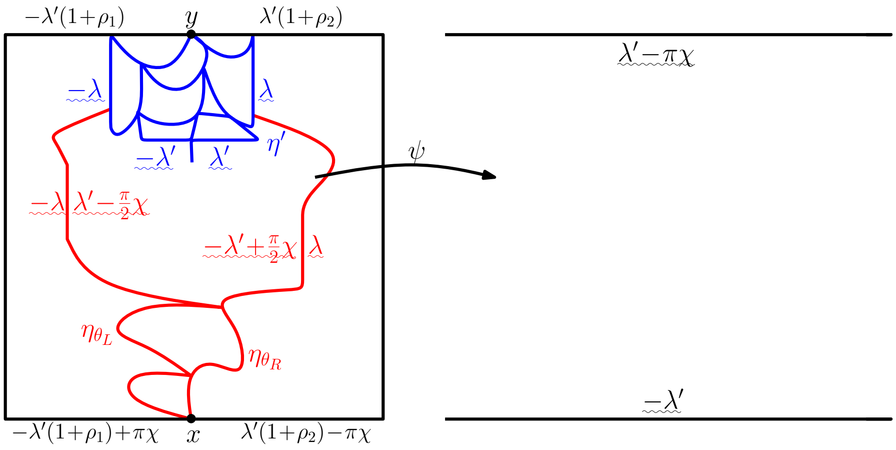

Figure 2.7: (Continuation of Figure 2.6). We now assume that the boundary data for h is as depicted above and that $\rho_1, \rho_2 > \frac{\kappa'}{2} - 4$. Then $\eta' \sim \mathrm{SLE}_{\kappa'}(\rho_1; \rho_2)$. Let η_{θ_L} and η_{θ_R} be the left and right boundaries of the counterflow line η', respectively. One can check that in this case, $\eta_{\theta_q} \sim \mathrm{SLE}_\kappa(\rho_1^q; \rho_2^q)$ with $\rho_1^q, \rho_2^q > -2$ for $q \in \{L, R\}$ (see Figure 2.3 and recall the transformation rule (2.5)). Each connected component C of $D \setminus (\eta_{\theta_L} \cup \eta_{\theta_R})$ which lies between η_{θ_L} and η_{θ_R} has two distinguished points x_C and y_C — the first and last points on ∂C traced by η_{θ_L} (as well as by η_{θ_R}). In each such C, the law of η' is independently an $\mathrm{SLE}_{\kappa'}(\frac{\kappa'}{2} - 4; \frac{\kappa'}{2} - 4)$ process from y_C to x_C [15, Proposition 7.30]. If we apply a conformal change of coordinates $\psi \colon C \to \mathcal{S}$ with $\psi(x_C) = -\infty$ and $\psi(y_C) = \infty$, then the law of $h \circ \psi^{-1} - \chi \arg(\psi^{-1})'$ is a GFF on $\mathcal{S}$ whose boundary data is depicted on the right hand side. Moreover, $\psi(\eta')$ is the counterflow line of this field running from $+\infty$ to $-\infty$ and almost surely hits every point on $\partial\mathcal{S}$. This holds more generally whenever the boundary data is such that $\eta_{\theta_L}, \eta_{\theta_R}$ make sense as flow lines of h until terminating at y (i.e., the continuation threshold it not hit until the process terminates at y).

of angle restricted SLE_κ trajectories in the same imaginary geometry [15, Theorem 1.4].

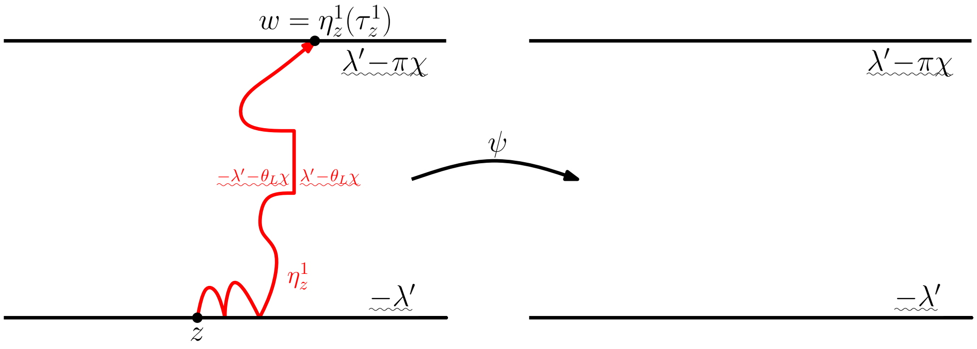

Figure 2.8: Suppose that h is a GFF on $\mathcal{S}$ whose boundary data is depicted above and fix z in the lower boundary $\partial_L\mathcal{S}$ of $\mathcal{S}$. Then the counterflow line η' of h from ∞ to $-\infty$ is an $\text{SLE}_{\kappa'}(\frac{\kappa'}{2}-4;\frac{\kappa'}{2}-4)$ process (see Figure 2.3 and recall the transformation rule (2.5)) and almost surely hits z, say at time τ_z'. The left boundary of $\eta'([0,\tau_z'])$ is almost surely equal to the flow line η_z^1 of h starting at z with angle $\theta_L=\frac{\pi}{2}$ stopped at time τ_z^1, the first time it hits the upper boundary $\partial_U\mathcal{S}$ of $\mathcal{S}$. The conditional law of h given $\eta_z^1([0,\tau_z^1])$ in each connected component of $\mathcal{S}\setminus\eta_z^1([0,\tau_z^1])$ which lies to the right of $\eta_z^1([0,\tau_z^1])$ is the same as h itself, up to a conformal change of coordinates which preserves the entrance and exit points of η'. The conditional law of η' within each such component is independently that of an $\text{SLE}_{\kappa'}(\frac{\kappa'}{2}-4;\frac{\kappa'}{2}-4)$ from the first to last endpoint [15, Proposition 7.32].

3 Proofs

In this section, we will complete the proofs of Theorems 1.1–1.3. The strategy for the former two is first to reduce the reversibility of $\text{SLE}_{\kappa'}(\rho_1;\rho_2)$ for $\rho_1,\rho_2\geq\frac{\kappa'}{2}-4$ to the reversibility of $\text{SLE}_{\kappa'}(\frac{\kappa'}{2}-4;\frac{\kappa'}{2}-4)$ (Lemma 3.1). The main step to establish the reversibility in this special case is Lemma 3.2, which implies that the law of the geometry of the outer boundary of the set of points visited by such a curve before and after hitting a particular boundary point z is invariant under the anti-conformal map which swaps the seed and terminal point but fixes z (see Figure 2.9). This allows us to construct a coupling of two $\text{SLE}_{\kappa'}(\frac{\kappa'}{2}-4;\frac{\kappa'}{2}-4)$ processes growing in opposite directions whose outer boundary before and after hitting z is the same. Successively iterating this exploration procedure in the complementary components results in a coupling where one path is almost surely the time-

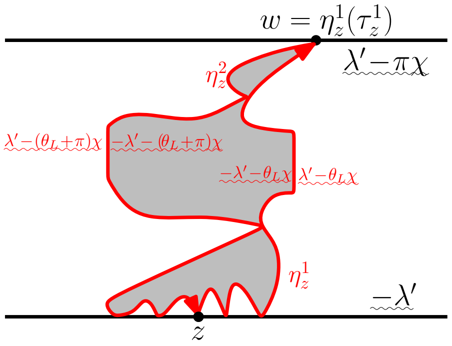
$w = \eta_z^1(\tau_z^1)$
η_z^2
$\lambda' - \pi\chi$
$\lambda' - (\theta_L + \pi)\chi$
$-\lambda' - (\theta_L + \pi)\chi$
$-\lambda' - \theta_L\chi$
$\lambda' - \theta_L\chi$
η_z^1
$-\lambda'$
z

Figure 2.9: (Continuation of Figure 2.8) Moreover, $\eta'([\tau_z', \infty))$ almost surely stays to the left of $\eta_z^1([0, \tau_z^1])$. It is the counterflow line of h restricted to the left component of $\mathcal{S} \setminus \eta_z^1([0, \tau_z^1])$, starting at z and running to $-\infty$ [15, Proposition 7.32]. Let $w = \eta_z^1(\tau_z^1)$. Since η' is boundary filling and cannot enter into the loops it creates with itself or the boundary, the first point on $\partial_U \mathcal{S}$ that η' hits after time τ_z' is w. The left boundary of $\eta'|_{[\tau_z', \infty)}$ is given by the flow line η_z^2 of h given $\eta_z^1([0, \tau_z^1])$ in the left connected component of $\mathcal{S} \setminus \eta_z^1([0, \tau_z^1])$ with angle θ_L, started at w and stopped at the time τ_z^2 that it first hits z. The order in which η' hits the connected components of $\mathcal{S} \setminus (\eta_z^1([0, \tau_z^1]) \cup \eta_z^2([0, \tau_z^2]))$ which lie to the right of $\eta_z^1([0, \tau_z^1])$ is determined by the reverse chronological order that η_z^1 traces their boundary. Likewise, the order in which η' hits those connected components which lie to the left of $\eta_z^2([0, \tau_z^2])$ is determined by the reverse chronological order that η_z^2 traces their boundary [15, Proposition 7.32]. Lemma 3.2 states that the law of the pair $\{\eta_z^1|_{[0, \tau_z^1]}, \eta_z^2|_{[0, \tau_z^2]}\}$ is invariant under reflection about the vertical axis through z up to time-reversal and reparameterization. This is a necessary condition for η' to be reversible.

reversal of the other, which completes the proof of reversibility. The proof of Lemma 3.2 will make use of the reversibility of $\text{SLE}_\kappa(\rho_1; \rho_2)$ [16, Theorem 1.1] and the "light cone" characterization of $\text{SLE}_{\kappa'}$ from [15, Theorem 1.4]. We will in particular need the variant of SLE duality described in Figure 2.8 and in Figure 2.9 (see [15, Section 7.4.3]) .

3.1 Reducing Theorems 1.1 and 1.2 to critical case

We begin with the reduction of Theorem 1.2 to the critical boundary-filling case, which was mostly explained in Figure 1.1.

Lemma 3.1. *Fix* $\rho_1, \rho_2 \geq \frac{\kappa'}{2} - 4$. *The reversibility of* $\mathrm{SLE}_{\kappa'}(\rho_1; \rho_2)$ *is equivalent to the reversibility of* $\mathrm{SLE}_{\kappa'}(\frac{\kappa'}{2} - 4; \frac{\kappa'}{2} - 4)$.

Proof. Suppose that D is a Jordan domain and $x, y \in \partial D$ are distinct. Assume that $\rho_1, \rho_2 > \frac{\kappa'}{2} - 4$ and let η' be an $\mathrm{SLE}_{\kappa'}(\rho_1; \rho_2)$ from y to x. Let $\psi \colon D \to D$ be an anti-conformal map which swaps x and y. Figure 2.7 implies that the left boundary η_L of η' is an $\mathrm{SLE}_\kappa(\rho_1^L; \rho_2^L)$ process from x to y for some $\rho_1^L, \rho_2^L > -2$. Since the time-reversal of η_L is an $\mathrm{SLE}_\kappa(\rho_2^L; \rho_1^L)$ process from y to x [16, Theorem 1.1], it follows that $\psi(\eta_L)$ has the law of the left boundary of an $\mathrm{SLE}_{\kappa'}(\rho_1; \rho_2)$ process in D from y to x. Combining Figure 2.7 with Figure 2.4, we see that the right boundary η_R of η' conditional on η_L is also an $\mathrm{SLE}_\kappa(\rho_1^R; \rho_2^R)$ process for $\rho_1^R, \rho_2^R > -2$ from x to y. Thus [16, Theorem 1.1] implies that the time-reversal of η_R given η_L is an $\mathrm{SLE}_\kappa(\rho_2^R; \rho_1^R)$ process from y to x. Consequently, we have that $\psi(\{\eta_L, \eta_R\})$ has the law of the outer boundary of an $\mathrm{SLE}_{\kappa'}(\rho_1; \rho_2)$ process in D from y to x. By Figure 2.7 (and [15, Proposition 7.30]), we know that the conditional law of η' given η_L and η_R is an $\mathrm{SLE}_{\kappa'}(\frac{\kappa'}{2} - 4; \frac{\kappa'}{2} - 4)$ process independently in each of the connected components of $D \setminus (\eta_L \cup \eta_R)$ which lie between η_L and η_R. This proves the desired equivalence for $\rho_1, \rho_2 > \frac{\kappa'}{2} - 4$. The proof is analogous if either $\rho_1 = \frac{\kappa'}{2} - 4$ or $\rho_2 = \frac{\kappa'}{2} - 4$. ☐

3.2 Main lemma

For the remainder of this section, we shall make use of the following setup. Let $\mathcal{S} = \mathbf{R} \times (0, 1)$ be the infinite horizontal strip in $\mathbf{C}$ and let h be a GFF on $\mathcal{S}$ whose boundary data is as indicated in Figure 2.9. Let $\partial_L \mathcal{S}$ and $\partial_U \mathcal{S}$ denote the lower and upper boundaries of $\mathcal{S}$, respectively. Fix $z \in \partial_L \mathcal{S}$ and let η_z^1 be the flow line of h starting at z with angle $\theta_L := (\lambda - \lambda')/\chi = \frac{\pi}{2}$ — this is the flow line of $h + \theta_L \chi$ starting at z. Due to the choice of boundary data, η_z^1 almost surely hits $\partial_U \mathcal{S}$ (see Figure 2.5), say at time τ_z^1. Let η_z^2 be the flow line of h with angle θ_L starting from $w = \eta_z^1(\tau_z^1)$ in the left connected component of $\mathcal{S} \setminus \eta_z^1([0, \tau_z^1])$. Due to the choice of boundary data, η_z^2 almost surely hits $\partial_L \mathcal{S}$ at z (though it will hit $\partial_L \mathcal{S}$ first in other places, see Figure 2.5), say at time τ_z^2.

For each $a \in \mathbf{R}$, we let $\mathcal{R}_a \colon \mathbf{C} \to \mathbf{C}$ be the reflection of $\mathbf{C}$ about the vertical line through a. We will now prove that the law of $T_z = \{\eta_z^1|_{[0,\tau_z^1]}, \eta_z^2|_{[0,\tau_z^2]}\}$, as in Figure 2.9, is invariant under $\mathcal{R}_z$, up to time-reversal and reparameterization.

Lemma 3.2. *The law of T_z defined just above is invariant under $\mathcal{R}_z$, up to time-reversal and reparameterization.*

We note that $\mathcal{R}_z$ is the unique anti-conformal map $\mathcal{S} \to \mathcal{S}$ which fixes z and swaps $-\infty$ with $+\infty$. The proof begins with a half-plane version of the construction described in Figure 2.9 (as would be obtained by "zooming in near z") which we explain in Figure 3.1. We then consider a similar construction (using the same instance of the GFF) from a nearby point, as shown in Figure 3.2. The result follows from these constructions in a somewhat indirect but rather interesting way. It builds on time-reversal results for $\mathrm{SLE}_\kappa(\rho_1;\rho_2)$ processes [16, Theorem 1.1] (see also [32, 5]) while avoiding additional calculation.

Proof of Lemma 3.2. Suppose that h is a GFF on $\mathbf{H}$ with constant boundary data $c = -\lambda'$ as depicted in Figure 3.1 and Figure 3.2. The main construction in this proof actually makes sense for any c such that $c \leq -\lambda'$ and $c + \theta_L \chi > -\lambda$ (and we will make use of this fact later). For each $z \in \mathbf{R}$, we let η_z^1 be the flow line of h starting at z with angle θ_L. Note that η_z^1 is an $\mathrm{SLE}_\kappa(\frac{-c-\theta_L\chi}{\lambda} - 1; \frac{c+\theta_L\chi}{\lambda} - 1)$ process (see Figure 2.3). Our hypotheses on c imply that both

$$\frac{-c-\theta_L\chi}{\lambda} - 1 \geq \frac{\kappa}{2} - 2 \text{ and } \frac{c+\theta_L\chi}{\lambda} - 1 \leq -\frac{\kappa}{2} < \frac{\kappa}{2} - 2.$$

In the latter inequality, we used that $\kappa \in (2,4)$. Consequently, η_z^1 almost surely does not hit $(-\infty, z)$ but almost surely does intersect (z,∞) (see Figure 2.5 as well as [15, Remark 5.3]). Conditionally on η_z^1, we let η_z^2 be the flow line of h in the left connected component of $\mathbf{H} \setminus \eta_z^1$ starting at ∞ with angle θ_L. Then η_z^2 is an $\mathrm{SLE}_\kappa(\kappa-4; \frac{c+\theta_L\chi}{\lambda} - 1)$ process in the left connected component of $\mathbf{H} \setminus \eta_z^1$ from ∞ to z (see Figure 2.4 and Figure 2.3; note also that since $\kappa \in (2,4)$ we have that $\kappa - 4 > -2$). Therefore η_z^2 almost surely exits $\mathbf{H}$ at z and cannot be continued further (though it may hit $\mathbf{R}$ in $(-\infty, z)$ before exiting; see Figure 2.5).

We let U_0 be the connected component of $\mathbf{H} \setminus (\eta_1^1 \cup \eta_1^2)$ which contains 0 on its boundary. Similarly, we let U_1 be the connected component of

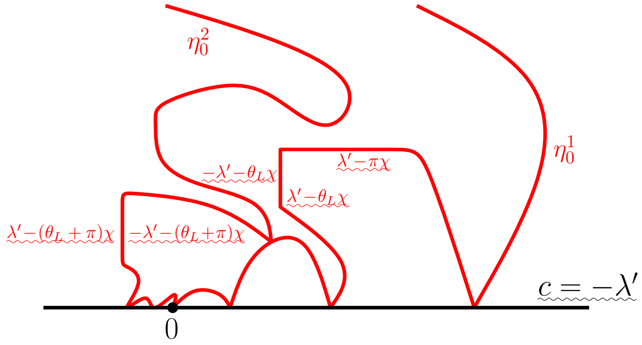

Figure 3.1: We consider the analog of Figure 2.9 in which $\mathcal{S}$ is replaced by the entire upper half plane $\mathbf{H}$. We let h be a GFF on $\mathbf{H}$ with constant boundary data $-\lambda'$ as depicted above. For $z \in \partial \mathbf{H}$, we let η_z^1 be the flow line of h with angle θ_L starting at z. Conditional on η_z^1, we let η_z^2 be the flow line of h with angle θ_L starting at ∞ in the left connected component of $\mathbf{H} \setminus \eta_z^1$. The particular case $z = 0$ is depicted above. In this case, the symmetry of the law of the pair of paths under reflection about the vertical line through 0 holds if and only if $c = -\lambda'$, as in the figure (Lemma 3.3). We will extract this from the time-reversal symmetry of $\mathrm{SLE}_\kappa(\rho_1;\rho_2)$ [16, Theorem 1.1]. The area between the pair of paths can be understood as a countable sequence of "beads". Some of these beads have boundaries that intersect the negative real axis, some the positive real axis, some neither axis, and some both axes (see Figure 2.5).

$\mathbf{H} \setminus (\eta_0^1 \cup \eta_0^2)$ which contains 1 on its boundary. Let $\psi_1 \colon U_1 \to \mathcal{S}$ be the conformal transformation, as indicated in Figure 3.2, which takes the left and rightmost points of $\mathbf{R} \cap \partial U_1$ to $-\infty$ and $+\infty$, respectively, and 1 to z. Let S_1 be the image of the restrictions of η_1^1 and η_1^2 to U_1. Given U_1, S_1 is equal in law to the bead sequence constructed in Figure 2.9 (see Figure 3.2). The same is also true for U_0 when we define S_0 analogously.

Note that $\mathcal{R}_{1/2}$ is an anti-conformal automorphism of $\mathbf{H}$ which swaps 0 and 1. Thus $\psi_1 \circ \mathcal{R}_{1/2}$ is an anti-conformal map from $\mathcal{R}_{1/2}(U_1)$ (which is a neighborhood of 0) to $\mathcal{S}$. Thus, Lemma 3.2 is a consequence of Lemma 3.4, stated and proved just below (and which uses $c = -\lambda'$). $\square$

Before we state and prove Lemma 3.4, we first need the following lemma which gives the reflection invariance of the pair of paths $T_z = \{\eta_z^1, \eta_z^2\}$ for

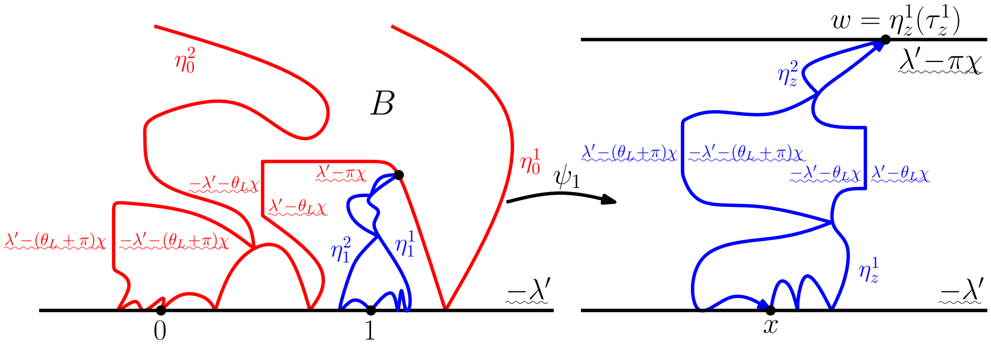
$w = \eta_z^1(\tau_z^1)$
$\lambda' - \pi\chi$
η_0^2
B
η_z^2
η_0^1
ψ_1
$\lambda' - (\theta_L + \pi)\chi$
$-\lambda' - (\theta_L + \pi)\chi$
$-\lambda' - \theta_L\chi$
$\lambda' - \theta_L\chi$
$\lambda' - \pi\chi$
$-\lambda' - \theta_L\chi$
$\lambda' - \theta_L\chi$
$\lambda' - (\theta_L + \pi)\chi$
$-\lambda' - (\theta_L + \pi)\chi$
η_1^2
η_1^1
η_z^1
$-\lambda'$
$-\lambda'$
0
1
x

Figure 3.2: (Continuation of Figure 3.1). The analogous sequence of beads beginning at 1 will at some point merge with the sequence beginning at 0 since their boundaries are given by flow lines with the same angle (see [15, Theorem 1.5]). Let B be the first bead that belongs to both sequences. In general, this bead may intersect any subset of the three intervals $(-\infty, 0)$, $(0,1)$, and $(1,\infty)$ (see Figure 2.5). (In the sketch above, it intersects both $(0,1)$ and $(1,\infty)$.) Let U_1 be the connected component of $\mathbf{H} \setminus (\eta_0^1 \cup \eta_0^2)$ which contains 1 and let $\psi_1 \colon U_1 \to \mathcal{S}$ be the conformal map which takes 1 to x, $x \in \partial_L \mathcal{S}$ fixed, and the left and right most points of $\partial U_1 \cap \mathbf{R}$ to $-\infty$ and ∞, respectively. Then $h \circ \psi_1^{-1} - \chi \arg(\psi_1^{-1})'$ is a GFF on $\mathcal{S}$ whose boundary data is as depicted on the right side, which is exactly the same as in Figure 2.9.

$z \in \partial\mathbf{H}$ (up to a time-reversal and reparameterization of the paths).

Lemma 3.3. *Suppose that h is a GFF on $\mathbf{H}$ with constant boundary data c with $c \in (-\lambda - \theta_L\chi, -\lambda']$. For each $z \in \mathbf{R}$, let η_z^1 be the flow line of h starting at z with angle θ_L. Conditionally on η_z^1, let η_z^2 be the flow line of h in the left connected component of $\mathbf{H} \setminus \eta_z^1$ from ∞ with angle θ_L. Then the law of the pair $\{\eta_z^1, \eta_z^2\}$ is invariant under $\mathcal{R}_z$ modulo direction reversing reparameterization if and only if $c = -\lambda'$.*

Proof. We first suppose that $c = -\lambda'$. By Figure 2.3 (see also the beginning of the proof of Lemma 3.2), we know that $\eta_z^1 \sim \mathrm{SLE}_\kappa(\frac{\kappa}{2} - 2; -\frac{\kappa}{2})$ and, conditionally on η_z^1, $\eta_z^2 \sim \mathrm{SLE}_\kappa(\kappa - 4; -\frac{\kappa}{2})$ from ∞ to z (the $\kappa - 4$ force point lies between η_z^2 and η_z^1). By the time-reversal symmetry of $\mathrm{SLE}_\kappa(\rho_1;\rho_2)$ processes [16, Theorem 1.1], this in turn implies that the law of the time-reversal $\mathcal{R}(\eta_z^2)$ of η_z^2 given η_z^1 is an $\mathrm{SLE}_\kappa(-\frac{\kappa}{2}; \kappa - 4)$ process from z to ∞ in the left connected component of $\mathbf{H} \setminus \eta_z^1$. By Figure 2.4, this in turn implies that

$\mathcal{R}(\eta_z^2)$ is an $\mathrm{SLE}_\kappa(-\frac{\kappa}{2}; \frac{\kappa}{2}-2)$ process from z to ∞ in $\mathbf{H}$ and, moreover, the law of η_z^1 given $\mathcal{R}(\eta_z^2)$ is an $\mathrm{SLE}_\kappa(\kappa-4; -\frac{\kappa}{2})$ process from z to ∞ in the right connected component of $\mathbf{H} \setminus \eta_z^1$. This proves the desired invariance of the law of $\{\eta_z^1, \eta_z^2\}$ under $\mathcal{R}_z$. For $c \neq -\lambda'$, the fact that the law of the pair $\{\eta_z^1, \eta_z^2\}$ is not invariant under $\mathcal{R}_z$ follows from a similar argument (recall the values of the weights ρ given in the beginning of the proof of Lemma 3.2). ☐

Lemma 3.4. *Suppose that h is a GFF on $\mathbf{H}$ with constant boundary data c with $c = -\lambda'$. For each $z \in \mathbf{R}$, let η_z^1 be the flow line of h starting at z with angle θ_L. Conditionally on η_z^1, let η_z^2 be the flow line of h in the left connected component of $\mathbf{H} \setminus \eta_z^1$ with angle θ_L from ∞ to z. For any $z, w \in \mathbf{R}$ with $z < w$, the law of $\{\eta_z^1, \eta_z^2, \eta_w^1, \eta_w^2\}$ is invariant under $\mathcal{R}_{(z+w)/2}$ (up to time-reversal and reparameterization).*

Proof. By rescaling and translating, we may assume without loss of generality that $z = 0$ and $w = 1$. For $a \in \{0, 1\}$, we let $T_a = \eta_a^1 \cup \eta_a^2$. We first observe that T_a is independent of S_{1-a} for $a \in \{0, 1\}$ (where we recall that S_a and U_a are defined in the proof of Lemma 3.2) and, by Lemma 3.3, we know that the law of T_a is invariant under $\mathcal{R}_a$.

We now consider the following rerandomization transition kernel $\mathcal{K}$. Based on the result of a fair coin toss, we either

1. Resample T_0 from its original law (leaving S_1 unchanged) and then resample T_1 from its original law (leaving S_0 unchanged).
2. Resample T_1 from its original law (leaving S_0 unchanged) and then resample T_0 from its original law (leaving S_1 unchanged)

Let $X_1 = T_0 \cup T_1$. Clearly, the law of X_1 is invariant under $\mathcal{K}$. Let Y_1 be the image of X_1 under $\mathcal{R}_{1/2}$. Since $\mathcal{K}$ is itself symmetric under $\mathcal{R}_{1/2}$, the law of Y_1 is also invariant under $\mathcal{K}$. We inductively define X_n and Y_n by applying $\mathcal{K}$ (using the same coin tosses and choices for new T_0 and T_1 values) to X_{n-1} and Y_{n-1}. Note that each X_n (resp. Y_n) has the same law as X_1 (resp. Y_1). Let K be the first time for which, during the rerandomization, we start by resampling T_0 and find that the first bead B which is contained in both T_0 and T_1 intersects both $(0, 1)$ and $(1, \infty)$, as depicted in Figure 3.2, and then we resample T_1. We note that this happens with positive probability in each application of $\mathcal{K}$. Clearly, $X_K = Y_K$ (since they have the same S_0 component after resampling T_0, and this remains true after the T_1 component is resampled for both). Thus $X_n = Y_n$ for all $n \geq K$ and K is almost surely finite. Thus X_1 and Y_1 must indeed have the same law as desired. ☐

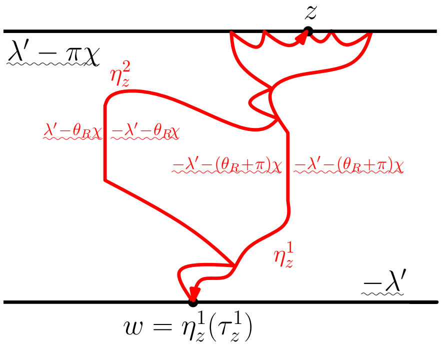
z
$\lambda' - \pi\chi$
η_z^2
$\lambda' - \theta_R\chi$
$-\lambda' - \theta_R\chi$
$-\lambda' - (\theta_R + \pi)\chi$
$-\lambda' - (\theta_R + \pi)\chi$
η_z^1
$-\lambda'$
$w = \eta_z^1(\tau_z^1)$

Figure 3.3: By symmetry, Figure 2.9 has an obvious "upside down" analog. Let h be a GFF on the infinite strip $\mathcal{S} = \mathbf{R} \times (0,1)$ in $\mathbf{C}$ with the boundary data depicted above. For $z \in \partial_U \mathcal{S}$, we let η_z^1 be the flow line of h with angle θ_R. Then η_z^1 has to hit the lower boundary $\partial_L \mathcal{S}$ of $\mathcal{S}$ (to see this, rotate the picture by 180 degrees, apply (2.5), and then Figure 2.5). Let w be the point where the path η_z^1 first hits $\partial_L \mathcal{S}$, say at time τ_z^1. Conditionally on $\eta_z^1([0,\tau_z^1])$, let η_z^2 be the flow line of h starting at w with angle θ_R in the left connected component of $\mathcal{S} \setminus \eta_z^1([0,\tau_z^1])$. Then η_z^2 almost surely exits $\partial_U \mathcal{S}$ at z, say at time τ_z^2 (see Figure 2.5). In analogy with Lemma 3.2, we have that the joint law of the pair $T_z = \{\eta_z^1|_{[0,\tau_z^1]}, \eta_z^2|_{[0,\tau_z^2]}\}$ is invariant under reflecting $\mathcal{S}$ about the vertical line through z (after time-reversal and reparameterization).

Remark 3.5. We can define T_z for $z \in \partial_U \mathcal{S}$ analogously and we have a reflection invariance result which is analogous to Lemma 3.2. This is described in Figure 3.3.

3.3 Iteration procedure exhausts curve

In view of Lemma 3.1 and Lemma 3.2, we can now complete the proof of Theorem 1.1 and Theorem 1.2.

Proof of Theorem 1.2. Let $D \subseteq \mathbf{C}$ be a bounded Jordan domain and fix $x, y \in \partial D$ distinct. We construct a sequence of couplings $(\eta'_{k,-}, \eta'_{k,+})$ of $\text{SLE}_{\kappa'}(\frac{\kappa'}{2} - 4; \frac{\kappa'}{2} - 4)$ curves on D with $\eta'_{k,-}$ connecting y to x and $\eta'_{k,+}$ connecting x to y as follows. We take $\eta'_{1,-}$ and $\eta'_{1,+}$ to be independent. Let $\mathcal{D}_1 = \{z_{n,1}\}$ be a countable, dense collection of points in ∂D and let $z_1 = z_{1,1}$. Lemma 3.2 implies that the law of $\overline{T}_{z_1}(\eta'_{1,-})$, the closure of the set of points

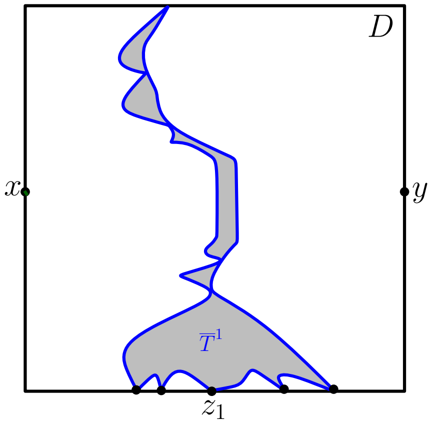

Figure 3.4: The first step in the coupling procedure used in the proof of Theorem 1.2 for $\rho_1 = \rho_2 = \frac{\kappa'}{2} - 4$. Let $(\eta'_{1,-}, \eta'_{1,+})$ be independent $\mathrm{SLE}_{\kappa'}(\frac{\kappa'}{2} - 4; \frac{\kappa'}{2} - 4)$ curves in a bounded Jordan domain D with $\eta'_{1,-}$ connecting y with x and $\eta'_{1,+}$ connecting x to y, $x, y \in \partial D$ distinct. Lemma 3.2 implies that the law of the set $\overline{T}_{z_1}(\eta_{1,-})$ which consists of the closure of the set of points which lie between the outer boundaries of $\eta'_{1,-}$ before and after hitting z_1 is equal in distribution to the corresponding set $\overline{T}_{z_1}(\eta'_{1,+})$ for $\eta'_{1,+}$. Therefore we can construct a coupling of $\mathrm{SLE}_{\kappa'}(\frac{\kappa'}{2} - 4; \frac{\kappa'}{2} - 4)$ processes $(\eta'_{2,-}, \eta'_{2,+})$ such that $\overline{T}^1 = \overline{T}_{z_1}(\eta'_{2,-}) = \overline{T}_{z_1}(\eta'_{2,+})$.

which lie between the outer boundaries of $\eta'_{1,-}$ before and after hitting z_1, is equal in law to the corresponding set $\overline{T}_{z_1}(\eta'_{1,+})$ for $\eta'_{1,+}$. Consequently, there exists a coupling $(\eta'_{2,-}, \eta'_{2,+})$ such that $\overline{T}^1 := \overline{T}_{z_1}(\eta'_{2,-}) = \overline{T}_{z_1}(\eta'_{2,+})$. Note that the order in which $\eta'_{2,-}$ visits the connected components of $D \setminus \overline{T}^1$ is the reverse of that of $\eta'_{2,+}$ [15, Proposition 7.32]. Moreover, the conditional law of $\eta'_{2,-}$ given $\overline{T}^1$ is independently an $\mathrm{SLE}_{\kappa'}(\frac{\kappa'}{2} - 4; \frac{\kappa'}{2} - 4)$ process in each of these components and likewise for $\eta'_{2,+}$ given $\overline{T}^1$ [15, Proposition 7.32].

We will now explain how to iterate this procedure. Let (d_j) be a sequence that traverses $\mathbf{N} \times \mathbf{N}$ in diagonal order, i.e. $d_1 = (1,1)$, $d_2 = (2,1)$, $d_3 = (1,2)$, etc. Suppose that $k \geq 2$. We inductively take $\mathcal{D}_k = \{z_{n,k}\}$ to be a countable, dense subset of $\partial \overline{T}^{k-1}$ and $z_k = z_{d_k}$. Applying Lemma 3.2 again, we know that $\overline{T}_{z_k}(\eta'_{k,-})$, the closure of the set of points which lie be-

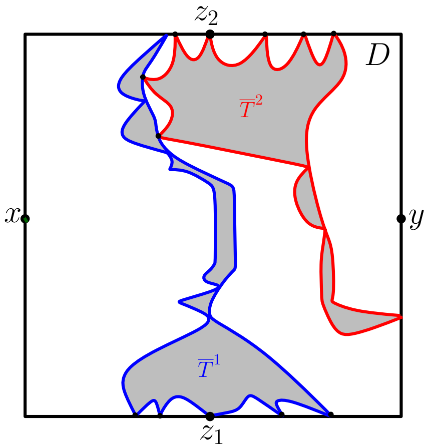

Figure 3.5: (Continuation of Figure 3.4). Suppose that $z_2 \in \partial D \setminus \overline{T}^1$. Then $\eta'_{2,-}$ and $\eta'_{2,+}$ are both $\text{SLE}_{\kappa'}(\frac{\kappa'}{2}-4;\frac{\kappa'}{2}-4)$ processes in the connected component C of $D \setminus \overline{T}^1$ which contains z_2 on its boundary. Applying Lemma 3.2 again thus implies that the law of the set $\overline{T}_{z_2}(\eta_{2,-})$ which consists of the closure of the set of points which lie between the outer boundaries of $\eta'_{2,-}$ before and after hitting z_2 is equal in distribution to the corresponding set $\overline{T}_{z_2}(\eta'_{2,+})$ for $\eta'_{2,+}$. Therefore we can construct a coupling of $(\eta'_{3,-},\eta'_{3,+})$ such that $\overline{T}^2 = \overline{T}_{z_2}(\eta'_{3,-}) = \overline{T}_{z_2}(\eta'_{3,+})$. The proof proceeds by successively coupling the boundary between the future and past of the two curves until one is almost surely the time-reversal of the other.

tween the outer boundaries of the set of points visited by $\eta'_{k,-}$ before and after hitting z_k, is equal in law to $\overline{T}_{z_k}(\eta'_{k,+})$, the corresponding set for $\eta'_{k,+}$. Thus by resampling $\eta'_{k,-}$ and $\eta'_{k,+}$ in the connected component of $D \setminus \cup_{j=1}^{k-1}\overline{T}^j$ with z_k on its boundary (and leaving the curves otherwise fixed), we can construct a coupling $(\eta'_{k+1,-},\eta'_{k+1,+})$ such that $\overline{T}^k := \overline{T}_{z_k}(\eta'_{k+1,-}) = \overline{T}_{z_k}(\eta'_{k+1,+})$ almost surely. Then the conditional law of $\eta'_{k+1,-}$ and $\eta'_{k+1,+}$ in each of the complementary components of $D \setminus \cup_{j=1}^{k}\overline{T}^j$ is independently that of an $\text{SLE}_{\kappa'}(\frac{\kappa'}{2}-4;\frac{\kappa'}{2}-4)$ process and $\eta'_{k+1,-}$ visits these connected components in the reverse order of $\eta'_{k+1,+}$ [15, Proposition 7.32].

To complete the proof, we will show that, up to reparameterization, the uniform distance of the time-reversal of $\eta'_{k,+}$ to $\eta'_{k,-}$ converges to 0 almost

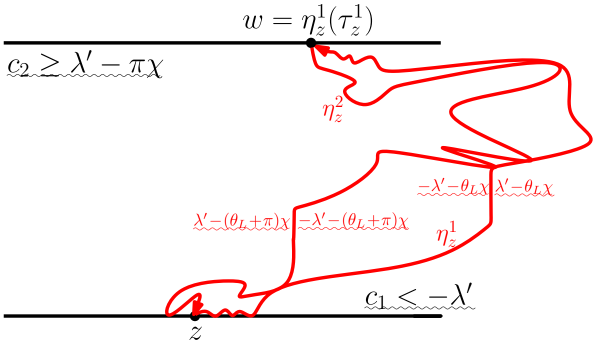
$w = \eta_z^1(\tau_z^1)$
$c_2 \geq \lambda' - \pi\chi$
η_z^2
$-\lambda' - \theta_L\chi$
$\lambda' - \theta_L\chi$
$\lambda' - (\theta_L + \pi)\chi$
$-\lambda' - (\theta_L + \pi)\chi$
η_z^1
$c_1 < -\lambda'$
z

Figure 3.6: The above figure illustrates what happens in the setting of Figure 2.9 when the constant upper and lower strip boundary data is modified so that the counter flow line η' from $+\infty$ to $-\infty$ is still boundary filling, but at least one of the ρ_i (say the one corresponding to the lower boundary) is strictly less than the critical value $\frac{\kappa'}{2} - 4$. As in Figure 2.9, the paths η_z^1 and η_z^2 describe the outer boundary of η' before and after hitting z. The law of the pair of paths in a neighborhood of z is absolutely continuous with respect to the law that one would obtain if the upper strip boundary were removed, so that both paths go between 0 and ∞ in $\mathbf{H}$ (and it is not hard to see that the local picture of the pair of paths converges to the half-plane picture upon properly rescaling). In this case, the "angle" between the right path and $(0, \infty)$ is less than that between the left path and $(-\infty, 0)$. Since the opposite is true for the reflected pair of paths (about the vertical line through z), the time-reversal of a boundary-filling $\mathrm{SLE}_\kappa(\rho_1; \rho_2)$ can only be an $\mathrm{SLE}_\kappa(\rho_1'; \rho_2')$ (for some ρ_1', ρ_2') if $\rho_1 = \rho_2 = \frac{\kappa'}{2} - 4$ (recall also Lemma 3.3).

surely. Note that $\eta_{k,-}' \stackrel{d}{=} \eta_{1,-}'$ and $\eta_{k,+}' \stackrel{d}{=} \eta_{1,+}'$ for all k. Consequently, the sequence $(\eta_{k,-}, \eta_{k,+})$ is tight (with respect to the topology induced by the uniform distance). Let (η_-, η_+) be any subsequential limit. Let $\mathcal{C}_k$ be the collection of connected components of $D \setminus \cup_{j=1}^k \overline{T}^j$. For $w \in D$, let $C_k(w)$ be the element of $\mathcal{C}_k$ which contains w (take $C_k(w) = \emptyset$ if there is no such connected component). Let $d_k = \mathrm{diam}(C_k(w))$, where we take $d_k = 0$ if $C_k(w) = \emptyset$. It suffices to show that $\lim_{k \to \infty} d_k = 0$ almost surely (the limit exists since d_k is decreasing). Let σ_k' be the time that η_-' enters $C_k(w)$ and let τ_k' be the time that η_-' leaves (by the construction, these are also the same times that $\eta_{j,-}'$ enters and leaves $C_k(w)$ for all $j > k$). By the continuity of η_-', it suffices to show that $\lim_{k \to \infty}(\tau_k' - \sigma_k') = 0$ almost surely (the limit exists because the sequence is monotonically decreasing). There exists $z \in (\mathcal{D}_1 \cup \cdots \cup \mathcal{D}_k) \cap \partial C_k(w)$ such that

$$|\eta'_-(\sigma'_k) - z| + |\eta'_-(\tau'_k) - z| \geq \tfrac{1}{2} d_k$$

since $(\mathcal{D}_1 \cup \cdots \cup \mathcal{D}_k) \cap \partial C_k(w)$ is dense in $\partial C_k(w)$. This implies that, with $\xi'_k = \inf\{t \in [\sigma'_k, \tau'_k] : \eta'_-(t) = z\}$ (recall that η'_- almost surely has to hit z since it fills the boundary of $C_k(w)$), we have either $\omega(|\xi'_k - \sigma'_k|) \geq \frac{1}{4} d_k$ or $\omega(|\tau'_k - \xi'_k|) \geq \frac{1}{4} d_k$ where ω is the modulus of continuity of η'_-. Using the notation of the previous paragraph, we have that $z = z_{j(k)}$ for some $j(k) > k$. By the construction, we have $[\sigma'_{j(k)}, \tau'_{j(k)}]$ is contained in either $[\sigma'_k, \xi'_k]$ or $[\xi'_k, \tau'_k]$. In the former case, we have

$$|\sigma'_{j(k)} - \tau'_{j(k)}| \leq |\sigma'_k - \tau'_k| - |\xi'_k - \tau'_k| \leq |\sigma'_k - \tau'_k| - \omega^{-1}(\tfrac{1}{4} d_k).$$

Similarly, in the latter case,

$$|\sigma'_{j(k)} - \tau'_{j(k)}| \leq |\sigma'_k - \tau'_k| - |\sigma'_k - \xi'_k| \leq |\sigma'_k - \tau'_k| - \omega^{-1}(\tfrac{1}{4} d_k).$$

This leads to a contradiction if $\lim_{k \to \infty} d_k \neq 0$ and therefore $\lim_{k \to \infty} d_k = 0$, almost surely, as desired. ☐

3.4 Non-critical boundary-filling paths

We now prove Theorem 1.3, which states that $\mathrm{SLE}_{\kappa'}(\rho_1; \rho_2)$ does not have time-reversal symmetry when $\min(\rho_1, \rho_2) < \frac{\kappa'}{2} - 4$.

Proof of Theorem 1.3. We may assume without loss of generality that $\rho_1 \in (-2, \frac{\kappa'}{2} - 4)$. This case is treated in Figure 3.6, together with the discussion of the half-plane problem for general constant boundary values c that was given in the proofs of Lemma 3.2 and Lemma 3.3. ☐

4 Couplings

One interesting aspect of time-reversal theory is that it allows us to couple two Gaussian free fields h and $\widetilde{h}$ with different boundary conditions in such a way that their difference is almost surely piecewise harmonic. In fact, for special choices of boundary conditions, one can arrange so that this difference is almost surely piecewise constant, with the boundary between

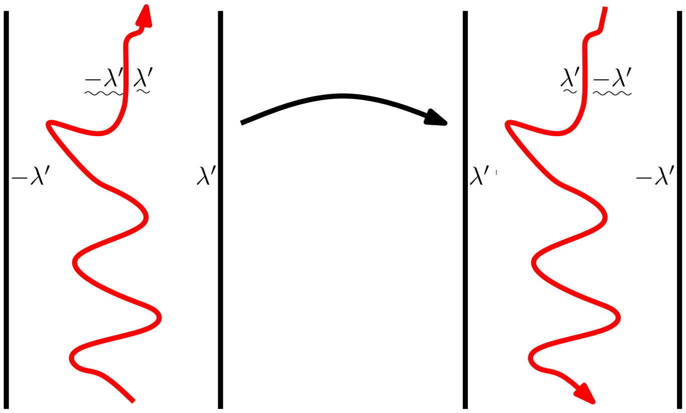

Figure 4.1: Consider a GFF h on the infinite vertical strip $[-1,1]\times\mathbf{R}$ whose boundary values are depicted on the left side above. The flow line η of h from the bottom to the top is an $\mathrm{SLE}_\kappa(\rho^L;\rho^R)$ process with $\rho^L=\rho^R=\frac{\kappa}{2}-2$. To go from the left figure to the right figure, add the constant function $2\lambda'$ to left side of the strip minus the path and $-2\lambda'$ to the right side to obtain a new field $\widetilde{h}$ with the boundary conditions shown on the right. By the reversibility of $\mathrm{SLE}_\kappa(\rho^L;\rho^R)$ processes [16, Theorem 1.1], $\widetilde{h}$ is a GFF with the boundary data indicated on the right side and the time-reversal of η is a flow line of $\widetilde{h}$ from the top to the bottom. Note that $h-\widetilde{h}$ is piecewise constant, equal to $-2\lambda'$ to the left of the path and $2\lambda'$ to the right. (We have not defined the difference on the almost surely zero-Lebesgue measure path η, but this does not effect the interpretation of this difference as a random distribution.)

constant regions given by an appropriate $\mathrm{SLE}_\kappa(\rho^L;\rho^R)$ curve. We illustrate this principle for flow lines in Figure 4.1, which we recall from [16].

The expectation field $E(z) := (\mathbf{E}(h-\widetilde{h}))(z)$ where h and $\widetilde{h}$ are as in Figure 4.1 is a linear function equal to $-2\lambda'$ on the left boundary of the strip and $2\lambda'$ on the right boundary. If we write $P_L(z)$ for the probability that z is to the left of the curve and $P_R(z)=1-P_L(z)$ for the probability that z is to the right, then $E(z)=-2\lambda' P_L(z)+2\lambda' P_R(z)$, which implies that $P_L(z)$ is a linear function equal to 1 on the left boundary of the strip and 0 on the right boundary.

In light of the results of this paper, one can produce a variant of Figure 4.1 involving counterflow lines when $\kappa\in(2,4)$ so that $\kappa'\in(4,8)$. We illustrate this in Figure 4.2. In this case, the expectation field $E(z) := (\mathbf{E}(h-\widetilde{h}))(z)$

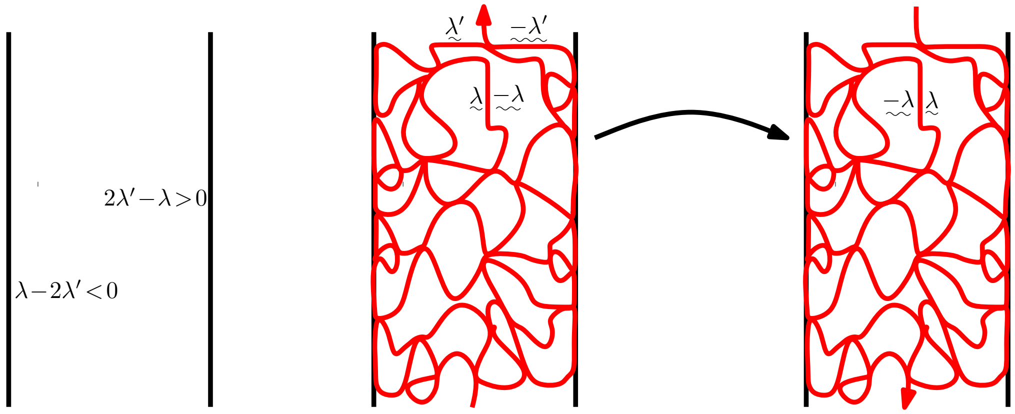

Figure 4.2: Consider a GFF h on the infinite vertical strip $[-1,1] \times \mathbf{R}$ whose boundary values are depicted on the left above. The counterflow line η' of h from the bottom to the top depicted in the middle above is an $\mathrm{SLE}_\kappa(\rho^L;\rho^R)$ process with $\rho^L = \rho^R = \frac{\kappa'}{2} - 4$. To see this, we note that $2\lambda' - \lambda = \lambda' - \frac{\pi}{2}\chi$ and $\lambda - 2\lambda' = -\lambda' + \frac{\pi}{2}\chi$. Consequently, if ψ is the conformal map which rotates the strip 90 degrees in the counterclockwise direction, the coordinate change formula (2.5) implies that the boundary conditions of the GFF $h \circ \psi^{-1} - \chi \arg(\psi^{-1})'$ agree with those of the GFF on the horizontal strip as depicted in Figure 2.8. This is a path that is boundary filling but not space filling and it divides the strip into countably many regions that lie "left" of the path and countably many that lie "right" of the path. As in Figure 4.1, we can go from the middle to the right figure by adding -2λ to the left side of the path and 2λ to the right side of the path. By the reversibility of $\mathrm{SLE}_\kappa(\rho^L;\rho^R)$ processes, the resulting field $\widetilde{h}$ is a GFF with the boundary data equal to -1 times the boundary data in the left figure, and the time-reversal of η' is the flow line of $\widetilde{h}$ from the top to the bottom. Note that $h - \widetilde{h}$ is piecewise constant, equal to 2λ on the left of the path and -2λ on the right.

is a linear function equal to $2(\lambda - 2\lambda') < 0$ on the left and $2(2\lambda' - \lambda) > 0$ on the right. If we define $P_L(z)$ and $P_R(z)$ as above, then in this setting we have $E(z) = 2\lambda P_L(z) - 2\lambda P_R(z)$. This implies that P_L is a linear function equal to $\frac{2(\lambda-2\lambda')+2\lambda}{4\lambda} = 1 - \lambda'/\lambda = (4-\kappa)/4 \in (0,1/2)$ on the left side and 1 minus this value, which is $\kappa/4 \in (1/2,1)$, on the right side.

At first glance it is counterintuitive that points near the left boundary are more likely to be on the right side of the path. This is the opposite of what we saw in Figure 4.1. To get some intuition about this, consider the extreme case that κ' and κ are very close to 4. In this case, the ρ^L and ρ^R values in Figure 4.2 are very close to -2, which means, intuitively, that when $\eta(t)$ is on the left side of the strip, it traces very closely along a long segment of the left boundary before (at some point) switching over to the right side and tracing a long segment of that boundary, etc. Given this intuition, it is not so surprising that points near the left boundary are more likely to be to the right of the path. When κ' is close to 8 (so that the counterflow line is close to being space filling) P_L and P_R are close to the constant function $\frac{1}{2}$. Here the intuition is that the path is likely to get very near to any given point z, and once it gets near it has a roughly equal chance of passing z to the left or right.

References

[1] G. Ben Arous and J.-D. Deuschel. The construction of the $(d+1)$-dimensional Gaussian droplet. *Comm. Math. Phys.*, 179(2):467–488, 1996.

[2] Federico Camia and Charles M. Newman. Two-dimensional critical percolation: the full scaling limit. *Comm. Math. Phys.*, 268(1):1–38, 2006.

[3] D. Chelkak and S. Smirnov. Universality in the 2D Ising model and conformal invariance of fermionic observables. *Invent. Math.*

[4] Julien Dubédat. Commutation relations for Schramm-Loewner evolutions. *Comm. Pure Appl. Math.*, 60(12):1792–1847, 2007.

[5] Julien Dubédat. Duality of Schramm-Loewner evolutions. *Ann. Sci. Éc. Norm. Supér. (4)*, 42(5):697–724, 2009.

[6] Julien Dubédat. SLE and the free field: partition functions and couplings. *J. Amer. Math. Soc.*, 22(4):995–1054, 2009.

[7] Christian Hagendorf, Denis Bernard, and Michel Bauer. The Gaussian free field and SLE_4 on doubly connected domains. *J. Stat. Phys.*, 140(1):1–26, 2010.

[8] K. Izyurov and K. Kytölä. Hadamard's formula and couplings of SLEs with free field. *ArXiv e-prints*, June 2010.

[9] R. Kenyon. Dominos and the Gaussian free field. *Annals of Probability*, 29:1128–1137, 2001.

[10] Gregory F. Lawler. *Conformally invariant processes in the plane*, volume 114 of *Mathematical Surveys and Monographs*. American Mathematical Society, Providence, RI, 2005.

[11] Gregory F. Lawler, Oded Schramm, and Wendelin Werner. Conformal invariance of planar loop-erased random walks and uniform spanning trees. *Ann. Probab.*, 32(1B):939–995, 2004.

[12] Nikolai Makarov and Stanislav Smirnov. Off-critical lattice models and massive SLEs. pages 362–371, 2010.

[13] J. Miller. Fluctuations for the Ginzburg-Landau model on a bounded domain. 2010.

[14] J. Miller. Universality for SLE(4). 2010.

[15] J. Miller and S. Sheffield. Imaginary Geometry I: interacting SLE paths. 2012.

[16] J. Miller and S. Sheffield. Imaginary Geometry II: reversibility of $\mathrm{SLE}_\kappa(\rho_1;\rho_2)$ for $\kappa \in (0,4)$. 2012.

[17] Ali Naddaf and Thomas Spencer. On homogenization and scaling limit of some gradient perturbations of a massless free field. *Comm. Math. Phys.*, 183(1):55–84, 1997.

[18] Brian Rider and Bálint Virág. The noise in the circular law and the Gaussian free field. *Int. Math. Res. Not. IMRN*, (2):Art. ID rnm006, 33, 2007.

[19] Steffen Rohde and Oded Schramm. Basic properties of SLE. *Ann. of Math. (2)*, 161(2):883–924, 2005.

[20] O. Schramm and S. Sheffield. A contour line of the continuum Gaussian free field. *ArXiv e-prints*, August 2010.

[21] Oded Schramm. Scaling limits of loop-erased random walks and uniform spanning trees. *Israel J. Math.*, 118:221–288, 2000.

[22] Oded Schramm. A percolation formula. *Electron. Comm. Probab.*, 6:115–120 (electronic), 2001.

[23] Oded Schramm and Scott Sheffield. Harmonic explorer and its convergence to SLE_4. *Ann. Probab.*, 33(6):2127–2148, 2005.

[24] Oded Schramm and Scott Sheffield. Contour lines of the two-dimensional discrete Gaussian free field. *Acta Math.*, 202(1):21–137, 2009.

[25] S. Sheffield. Local sets of the Gaussian free field: slides and audio. www.fields.utoronto.ca/0506/percolationsle/sheffield1, www.fields.utoronto.ca/audio/0506/percolationsle/sheffield2, www.fields.utoronto.ca/audio/0506/percolationsle/sheffield3.

[26] S. Sheffield. Conformal weldings of random surfaces: SLE and the quantum gravity zipper. *ArXiv e-prints*, December 2010.

[27] S. Sheffield and W. Werner. Conformal Loop Ensembles: The Markovian characterization and the loop-soup construction. *ArXiv e-prints*, June 2010.

[28] Scott Sheffield. Exploration trees and conformal loop ensembles. *Duke Math. J.*, 147(1):79–129, 2009.

[29] Stanislav Smirnov. Critical percolation in the plane: conformal invariance, Cardy's formula, scaling limits. *C. R. Acad. Sci. Paris Sér. I Math.*, 333(3):239–244, 2001.

[30] Stanislav Smirnov. Conformal invariance in random cluster models. I. Holomorphic fermions in the Ising model. *Ann. of Math. (2)*, 172(2):1435–1467, 2010.

[31] Wendelin Werner. Random planar curves and Schramm-Loewner evolutions. In *Lectures on probability theory and statistics*, volume 1840 of *Lecture Notes in Math.*, pages 107–195. Springer, Berlin, 2004.

[32] Dapeng Zhan. Reversibility of chordal SLE. *Ann. Probab.*, 36(4):1472–1494, 2008.

[33] Dapeng Zhan. Reversibility of some chordal SLE($\kappa;\rho$) traces. *J. Stat. Phys.*, 139(6):1013–1032, 2010.

Microsoft Research
One Microsoft Way
Redmond, WA, USA

Department of Mathematics
Massachusetts Institute of Technology
Cambridge, MA, USA